The coexistence of magnetic and superconducting phases in TmNi$_2$B$_2$C

Jens Jensen

Ørsted Laboratory, Niels Bohr Institute fAPG, Universitetsparken 5, 2100 Copenhagen, Denmark

(February, 2000)

I. MAGNETIC PROPERTIES

The Tm-ions in TmNi$_2$B$_2$C are placed in a body-centered tetragonal lattice with the lattice parameters [1]: $a = 3.4866$ Å and $c = 10.5860$ Å corresponding to $N(\text{Tm}) = 1.55415 \cdot 10^{22}$ cm^{-3}. The crystal-field Hamiltonian is defined in terms of five parameters:

$$\mathcal{H}_{\text{CF}} = \sum_{l=2,4,6} B_{l0} O_l^0 + \sum_{l=4,6} B_l^4 O_l^4 \qquad (1)$$

where O_l^m are the Stevens operators. The parameters have been determined from the crystal-field levels observed by inelastic neutron scattering in combination with the fitting of the paramagnetic susceptibility and heat capacity measurements [2]. (The parameters in the Table 2 of Ref. [2] are not the CEF parameters A_{nm}, but are the Stevens parameters B_l^m divided by the Stevens factors α_l). The parameters used here have been adjusted slightly in comparison with those given in Ref. [2] in order to improve the fit to the susceptibility measurements (without much modifications of the neutron scattering cross section). The fit obtained is shown in Fig. 1, and the corresponding crystal-field parameters are given in Table I.
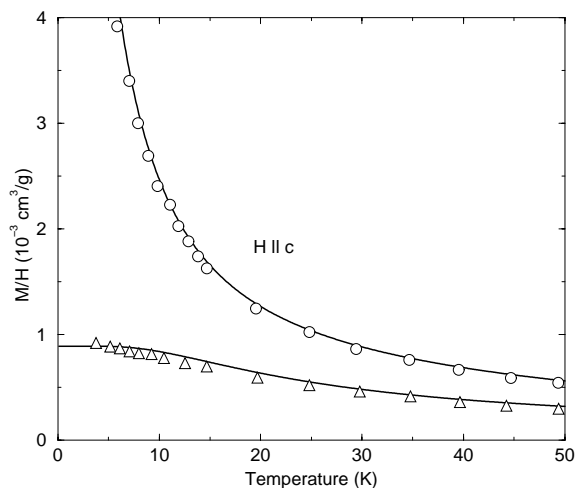
FIG. 1. The a- and c-axis susceptibilities of TmNi$_2$B$_2$C. The experimental results are taken from Ref. [3]. Corrections for the demagnetization fields have been made.

As shown in Fig. 1 these crystal-field parameters lead to a large difference between the two susceptibility components. The crystal-field level scheme has a doublet ground-state and only the J_z component has non-zero matrix elements within the two states. The next two excited states are nearly degenerated and lie 3.0 meV above the ground state. The present parameters lead to a saturation of the moments along the c-axis of 4.8 μ_B at 2 K and a field of 30 kOe, in close agreement with the value observed by Cho et $al.$ [3]. Under the same conditions the moments along an a-axis are 1.9 μ_B.

The two-ion interactions are assumed to be described effectively by a Heisenberg Hamiltonian:

$$\mathcal{H}_{\text{H}} = -\frac{1}{2} \sum_{i,j} \mathcal{J}(ij) \mathbf{J}_i \cdot \mathbf{J}_j \qquad (2)$$

The phase transition at $T_N = 1.52$ K at the wave vector $\mathbf{Q}_F = 0.094(\frac{2\pi}{a}, \frac{2\pi}{a}, 0)$, in the superconducting phase, determines

$$\mathcal{J}(\mathbf{Q}_F) = \frac{1}{\chi_0^{cc}(T_N)} = \frac{1}{116.3} \text{ meV} = 8.6 \ \mu\text{eV} \qquad (3)$$

$\chi_0^{cc}(T)$ is the cc-component of the non-interacting susceptibility determined by the crystal-field Hamiltonian at the temperature T [in units of $(g\mu_B)^2$]. The Fourier transform of $\mathcal{J}(ij)$ is defined in the usual way. The classical dipole coupling is of the same order of magnitude as the exchange coupling in TmNi$_2$B$_2$C. This coupling has been calculated in the present system using the method of Bowden and Clark [4], see Fig. 2. Most of the effects of this coupling are included in an effective fashion in the crystal-field and exchange parameters. For instance the rather large anisotropy at zero wave vector: $\mathcal{J}^{aa}(\mathbf{0}) - \mathcal{J}^{cc}(\mathbf{0}) = 9.15 \ \mu\text{eV}$ is accounted for by the crystal-field Hamiltonian (as this describes correctly the susceptibility components in the paramagnetic phase). The only dipole term which is included in an explicit way is the demagnetization field. The demagnetization field is at maximum ($g = 7/6$ and $J = 6$):

$$H_d^0 = 4\pi M_0 = 4\pi g\mu_B JN = 12.68 \text{ kOe} \qquad (4)$$

where M_0 is the saturation value of the amplitude of the magnetization vector:

$$\mathbf{M} = g\mu_B \frac{1}{V} \sum_i \langle \mathbf{J}_i \rangle \qquad (5)$$

TABLE I. The crystal-field parameters (meV).

B_2^0	B_4^0	B_4^4	B_6^0	B_6^4
-0.12	$0.33 \cdot 10^{-3}$	-0.01	$0.7 \cdot 10^{-5}$	$-1.16 \cdot 10^{-4}$
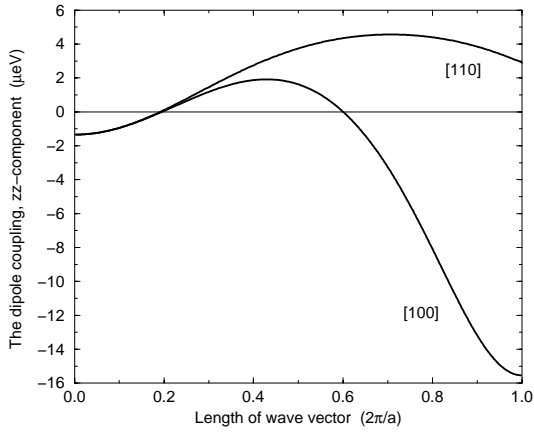
Fig. 2. The zz-component of the classical dipole coupling in the case of TmNi$_2$B$_2$C, when the wave vector is along [100] or [110]. Notice that this coupling adds 0.65 and 3.1 μeV to $\mathcal{J}(\mathbf{Q}) - \mathcal{J}(\mathbf{0})$, when $\mathbf{Q} = \mathbf{Q}_F$ and $\mathbf{Q} = \mathbf{Q}_A$, respectively.

The mean-field Hamiltonian for the ith ion is

$$\mathcal{H}_{\mathrm{MF}}(i) = \mathcal{H}_{\mathrm{CF}} - g\mu_B \mathbf{J}_i \cdot \mathbf{H}_i^{\mathrm{eff}} \qquad (6)$$

where

$$\mathbf{H}_i^{\mathrm{eff}} = \mathbf{H} - 4\pi D\mathbf{M} + \frac{1}{g\mu_B}\sum_j \mathcal{J}(ij)\langle \mathbf{J}_j\rangle \qquad (7)$$

$\mathbf{H}$ is the applied field and the demagnetization factor D is lying between 0 and 1. In most of the calculations $D^{zz} = 0.76$ and $D^{xx} = (1 - D^{zz})/2 = 0.12$, which are the values in the experiment of Cho et al. [3]. In a disk with diameter a and height b

$$D_\perp = \frac{1}{e^2}\left(1 - \frac{\sqrt{1-e^2}}{e}\sin^{-1} e\right) \quad ; \quad e = \sqrt{1 - \frac{b^2}{a^2}} \quad (8)$$

implying that the neutron-scattering samples have a c-axis demagnetization factor of 0.83 ± 0.3 (depending on how well the geometry of the sample, as for instance $6 \times 8 \times 1$, may be described by an ellipsoid).

The equilibrium state is found in an inductive way as the self-consistent solution of Eqs. (6) and (7) using

$$\langle \mathbf{J}_i\rangle = \frac{1}{Z(i)}\mathrm{Tr}\left(\mathbf{J}_i \exp[-\beta\mathcal{H}_{\mathrm{MF}}(i)]\right) \qquad (9)$$

$\beta = 1/k_B T$, and the partition function for the ith ion is

$$Z(i) = \mathrm{Tr}\left(\exp[-\beta\mathcal{H}_{\mathrm{MF}}(i)]\right) \qquad (10)$$

The traces are evaluated from the eigenvalues and eigenfunctions of the mean-field Hamiltonian using the EISPACK fortran subroutines. The free energy of the magnetic Hamiltonian is finally

$$F_{\mathrm{Mag}} = F_{\mathrm{MF}} + \frac{1}{2}\sum_{i,j}\mathcal{J}(ij)\langle \mathbf{J}_i\rangle \cdot \langle \mathbf{J}_j\rangle - \frac{1}{2}4\pi D\mathbf{M}^2$$

$$= \sum_i\left[-\frac{1}{\beta}\ln Z(i) + \frac{1}{2}g\mu_B\langle \mathbf{J}_i\rangle \cdot (\mathbf{H}_i^{\mathrm{eff}} - \mathbf{H})\right] \quad (11)$$

If, e.g., only the z component of $\langle \mathbf{J}_i\rangle$ is non-zero and is described by one harmonic, $\langle J_j^z\rangle = J_Q\cos(\mathbf{Q}\cdot\mathbf{R}_j + \phi)$ then the exchange contribution to $\mathbf{H}_i^{\mathrm{eff}}$ in Eq. (7) is $\mathcal{J}(\mathbf{Q})J_Q\cos(\mathbf{Q}\cdot\mathbf{R}_i + \phi)$. This expression shows that the most important factors in the determination of the free energy of the different modulated structures is the crystal-field parameters and the value of $\mathcal{J}(\mathbf{Q})$, and, in the presence of a ferromagnetic moment, of $\mathcal{J}(\mathbf{0})$. The actual values of the real-space exchange parameters $\mathcal{J}(ij)$ are of less significance. The squaring-up process introduces higher-order odd harmonics in the modulation of the moments, but even in the limit where the modulation is a square wave the third harmonic is three times smaller than the first one, and more than 80% of the free energy is still determined by the first harmonic. In the present system the ordering wave vectors are close to 0 or 1/2 in units of $2\pi/a$ implying that $\mathcal{J}(3\mathbf{Q})$ does not differ much from $\mathcal{J}(\mathbf{Q})$, therefore I expect that the unacquaintedness with the values of the exchange coupling at $(2n+1)\mathbf{Q}$ only gives rise to an uncertainty of less than 5% in the determination of the exchange energy. In the calculations I have assumed $\mathbf{Q} = 0.1(\frac{2\pi}{a}, \frac{2\pi}{a}, 0)$ corresponding to a commensurable structure along [1,1,0] with a period of 10 layers. This assumption implies an average of the free energy over 10 different values of the exchange field. The real-space coupling parameters used are:

$$\mathcal{J}_0 = \sum_{j\in i\text{'th layer}}\mathcal{J}(ij) = 6.798\ \mu\mathrm{eV},$$

$$\mathcal{J}_1 = \sum_{j\in (i+1)\text{'th layer}}\mathcal{J}(ij) = 1.264\ \mu\mathrm{eV},$$

$$\mathcal{J}_2 = \sum_{j\in (i+2)\text{'th layer}}\mathcal{J}(ij) = -0.392\ \mu\mathrm{eV}.$$

Introducing $\tilde{q}$, defined by $\mathbf{q} = \tilde{q}(\frac{2\pi}{a}, \frac{2\pi}{a}, 0)$ when $\mathbf{q}$ is along [1,1,0], then

$$\mathcal{J}(\tilde{q}) = \mathcal{J}_0 + 2\mathcal{J}_1\cos(2\pi\tilde{q}) + 2\mathcal{J}_2\cos(4\pi\tilde{q})$$

which has its maximum at $\tilde{q} = 0.1$, so that $\mathcal{J}(\tilde{q} = 0.1) = 8.6\ \mu\mathrm{eV}$ and $\mathcal{J}(\tilde{q} = 0) = 8.542\ \mu\mathrm{eV}$. The value of $\mathcal{J}(\mathbf{0})$ actual wanted in the Hamiltonian is incorporated by adjusting $\mathbf{H}_i^{\mathrm{eff}}$

$$\Delta\mathbf{H}_i^{\mathrm{eff}} = \left[\mathcal{J}(\mathbf{0}) - \mathcal{J}(\tilde{q} = 0)\right]\frac{1}{g\mu_B N}\sum_j\langle \mathbf{J}_j\rangle \qquad (12)$$

This same procedure, i.e. 10-layered structure, has been used for calculating the free energy of the ordered structure at $\mathbf{Q} = \mathbf{Q}_F$ and at $\mathbf{Q} = \mathbf{Q}_A = 0.482(\frac{2\pi}{a}, 0, 0)$, except that in the latter case the three exchange constants $\mathcal{J}_0$, $\mathcal{J}_1$ and $\mathcal{J}_2$ were scaled by one common fitting factor. The value of this parameter used in the final fit is 1.75 corresponding to

$$\mathcal{J}(\mathbf{Q}_A) = 15.0\ \mu\mathrm{eV}. \qquad (13)$$

II. SUPERCONDUCTING PROPERTIES

The superconducting transition temperature is $T_c = 11$ K corresponding to a superconducting energy gap at zero temperature $\Delta(0) = 1.764 k_B T_c = 1.7$ meV. One of the main results of this analysis is that the transition between the superconducting and the normal phase does not directly determine B_{c2}. Instead it is assumed that B_{c2} more or less behaves in the same way as in the "non-magnetic rare-earth" borocarbides (Y and Lu). The measurements of B_{c2} in LuNi$_2$B$_2$C [5] show $T_c = 16.5$ K and $B_{c2}(0) = 76$ kG, and they explain the temperature dependence of $B_{c2}(T)$ by a two-band model. Some differences between the electronic band-structures in the different rare-earth systems may be expected, but except for a scaling of T_c from 16.5 to 11 K and a similar scaling of $B_{c2}(0)$, the relative temperature dependence of $B_{c2}(T)$ is assumed to be the same in the Tm as in the Lu system. I have no special reason for choosing Lu rather than Y, except that fit produced by the two-band model is better in the first case than in the second. There are some differences between the two systems, and I start to wonder whether the Y behavior might not have been a better choice, but it is difficult to say. I have used the following cubic fit to the Lu-data in Ref. [5]:

$$B_{c2}(t) = B_{c2}(0)\left(1 - 0.285\,t - 2.196\,t^2 + 1.481\,t^3\right) \quad (14)$$

$t = T/T_c$ and in this expression I have used $T_c = 11.5$ K rather than 11 K (corresponding to a weak adjustment of the high temperature behavior). The measurements of Rathnayaka et al. [6] show that the anisotropy between the cases, where the field is applied parallel or perpendicular to the c axis, is very small, and in the final fit I have used

$$B_{c2}(0) = 65 \text{ kG} \quad (15)$$

in both cases. The value of the maximum field is a reasonable interpolation between the values observed in the cases of Y ($T_c = 15.7$ K; $B_{c2}(0) = 106$ kG) and Lu ($T_c = 16.5$ K; $B_{c2}(0) = 76$ kG), if assuming that the band-structure differences reduce $B_{c2}(0)$ with the same factor as T_c is reduced.

The new interpretation of the transition between the superconducting and the normal state implies that the analysis of this transition by Cho et al. [3] should be reconsidered. They determined the parameters $\kappa_\parallel = 6.3 \pm 0.3$ and $\kappa_\perp = 7.7 \pm 0.4$ by using the temperature derivative of the following expression

$$-4\pi M_s = \frac{H_{c2}(T) - H}{1.16 \cdot 4\pi(2\kappa^2 - 1)} \quad (16)$$

close to T_c assuming H_{c2} to be the same as the transition field H_{c2}'. From the calculations I have estimated that H_{c2}'/H_{c2} is close to 0.6 and 0.8 in the c- and a-axis cases, respectively. The theoretical estimates are rather uncertain close to T_c, however, if assuming them to be correct,

I find $\kappa_\parallel = 8.1 \pm 0.4$ and $\kappa_\perp = 8.6 \pm 0.5$. Within the uncertainties the two values are equal and the common value is $\kappa = 8.3$. On the other hand, the temperature derivative of the $B_{c2}(T)$ curve is not much different from the experimental values in the temperature regime considered, which suggests that the two scaling corrections made here may not be trusted. The estimate of the superconducting condensation energy (see below) may be utilized for a similar indirect determination of κ, and the value I deduce from the fit is $\kappa \simeq 6.3$ (in both cases). I think that this estimate of κ and those based on the measurements of Cho et al. are equally uncertain. The most qualified guess would be to use the average as a measure for κ

$$\kappa = \frac{\lambda}{\xi} = 7.3 \pm 1 \quad (17)$$

$\xi(0)$ is estimated from their values of $B_{c2}(0)$, and then λ is derived using the values of κ. With the new values of these parameters I obtain:

$$\xi(0) = \sqrt{\frac{\phi_0}{2\pi B_{c2}(0)}} = 71 \text{ Å} \quad ; \quad \lambda(0) = \kappa\xi(0) = 520 \text{ Å} \quad (18)$$

where $\phi_0 = 20.68 \cdot 10^8$ GÅ^2 is the flux quantum. Finally, we have

$$B_{c1} = \frac{\phi_0}{4\pi\lambda^2}\ln\kappa = 1.2 \text{ kG} \quad ; \quad B_c = \frac{B_{c2}}{\sqrt{2}\kappa} = 6.3 \text{ kG} \quad (19)$$

The condensation energy in the type II superconducting state is estimated using the Ginzburg-Landau expression for the free energy derived by Abrikosov, see for instance Ref. [7]. This is based on the integration of the linear field-dependent magnetization of the superconducting electrons (close to B_{c2} and T_c) given by Eq. (16)

$$F_s(T, B_i) - F_n = -\frac{(B_{c2}(T) - B_i)^2}{1.16 \cdot 8\pi(2\kappa_F^2 - 1)} \quad (20)$$

The field B_i is the field which the superconductor considers to be the external field (the internal field minus the contribution $4\pi M_s$ from the superconductor itself, when neglecting the demagnetization term due to M_s):

$$B_i = B + 4\pi(1 - D)M \quad (21)$$

where M is the magnetization of the Tm-ions, Eq. (5), and B is the applied field. The contribution of the Tm-ions to B_i is of the order of 10% in both the c- and the a-axis case [the moment induced in the a-axis case is somewhat smaller, but $(1 - D)$ is about a factor 5 larger than in the c-axis case]. At 2 K, in the c-axis case, I get $B_i/B = 1.12$ when $D = 0.83$, in nice agreement with the result shown by Morten in Fig. 22 in his thesis.

The free energy expression given by Eq. (20) is derived under the assumption that the order parameter is small (close to B_{c2}), but is used here in the total regime of the superconducting state. We expect that the quadratic dependence is a reasonable approximation, as long as the system is not in the Meissner phase, but the constant in front should not be taken too literally. Nevertheless, the constant derived from the final fit corresponds to $1.16(2\kappa_F^2 - 1) = 90$ or

$$\kappa_F = 6.27 \qquad (22)$$

where $\kappa_F = \kappa$ agrees reasonably well with the result of Cho *et al.*, as discussed above.
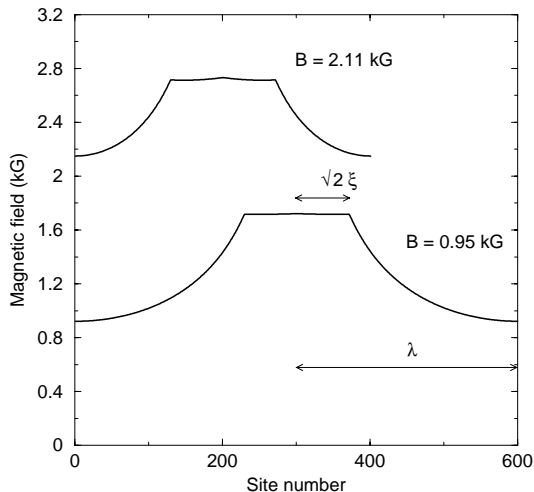
Fig. 3. The variation of the field around quadratic flux-lines placed in a cubic lattice. The results are along a line connecting two flux lines (periodic conditions) through one of the diagonal of the quadratic flux line. The cases shown correspond to $\xi = 128$ Å and $\kappa = 6.1$. The smaller value of $\xi = 71$ Å implies a scaling of the field values by $128/71$, which is reduced to some extent if κ is increased.

The model calculations are based on the most simplifying conditions. One of the assumptions made is that the field **H** in Eq. (7) and thus also the magnetization **M** is homogeneous throughout the sample. This is not true in the type-II phase where the field is truncated into the flux lines, however, the large value of κ implies a rather uniform field distribution: the variation is only about 10% at low temperatures at an averaged (applied) field of 4 kG, see Fig. 3. Finally, it may be mentioned that the magnetization due to the superconducting current, $4\pi M_s$, is at maximum a factor 10^3 smaller that B_{c2}, see Eq. (16), and thus negligible outside the Meissner phase.

III. THE INTERACTIONS BETWEEN THE MAGNETIC AND SUPERCONDUCTING ELECTRONS

The coupling between the magnetic and the superconducting systems is assumed to be as weak as it possibly can. The only effect considered is that the electrons which establish the indirect RKKY exchange-coupling between the Tm-ions, are metallic and share the Fermi surface with the electrons which condense into the superconducting state. In real space the two types of electrons may be quite isolated from each other.

The Heisenberg exchange-interaction between the conduction electrons and the localized $4f$ electrons gives rise to the indirect RKKY-coupling between the Tm ions mediated by the metallic electrons. The RKKY interaction of the Tm ions is determined by the susceptibility of the conduction electrons, $\chi_{\rm el}(\mathbf{q})$ (at zero frequency) [8]:

$$\mathcal{J}(\mathbf{q}) = \sum_{\boldsymbol{\tau}} |j(\mathbf{q} + \boldsymbol{\tau})|^2 \chi_{\rm el}(\mathbf{q} + \boldsymbol{\tau})$$
$$- \frac{1}{N} \sum_{\mathbf{q}'} \sum_{\boldsymbol{\tau}} |j(\mathbf{q}' + \boldsymbol{\tau})|^2 \chi_{\rm el}(\mathbf{q}' + \boldsymbol{\tau}) \qquad (23)$$

$j(\mathbf{q})$ is an exchange integral proportional to $(g-1)$, which may be assumed to vary slowly with $\mathbf{q}$, and $\boldsymbol{\tau}$ denotes a reciprocal lattice vector. The last term implies that the RKKY-interaction of the ith ion with itself is cancelled [as this interaction just adds a constant to the Hamiltonian, $\mathbf{J}_i \cdot \mathbf{J}_i = J(J+1)$]. In the free electron model (in the normal state), the susceptibility [per electron in units of $(g\mu_B)^2$] is:

$$\chi_{\rm el}(\mathbf{q}) = \frac{1}{2N} \sum_{\mathbf{k}} \frac{f(\epsilon_{\mathbf{k}}) - f(\epsilon_{\mathbf{k-q}})}{\epsilon_{\mathbf{k-q}} - \epsilon_{\mathbf{k}}} \quad ; \quad \chi_{\rm el}(\mathbf{0}) = \frac{1}{2}\mathcal{N}(0)$$
$$(24)$$

where $\mathcal{N}(0)$ is the density of state at the Fermi surface per electron and per spin state. The adding of a reciprocal wave vector to $\mathbf{q}$ or $\mathbf{k}$, as occurring in Eq. (23), corresponds in the band-electron picture to a change of the band index. Restricting $\mathbf{q}$ or $\mathbf{q}'$ in (23) to be wave vectors lying within the first Brillouin zone, then the terms with $\boldsymbol{\tau} = \mathbf{0}$ are the intra-band contributions, whereas the remaining ones are the inter-band terms corresponding to different band indices in Eq. (24).

Introducing the BCS energy gap Δ and the quasi-particle energy $E_{\mathbf{q}} = \sqrt{\epsilon_{\mathbf{q}}^2 + \Delta^2}$ then the susceptibility in the superconducting state is

$$\chi_{\rm el}^s(\mathbf{q}) = \frac{1}{2N} \sum_{\mathbf{k}} \frac{f(E_{\mathbf{k}}) - f(E_{\mathbf{k-q}})}{E_{\mathbf{k-q}} - E_{\mathbf{k}}}$$
$$+ \frac{1}{2N} \sum_{\mathbf{k}} \left[\frac{f(E_{\mathbf{k}}) - \frac{1}{2}}{E_{\mathbf{k}}} - \frac{f(E_{\mathbf{k-q}}) - \frac{1}{2}}{E_{\mathbf{k-q}}} \right]$$
$$\times \frac{E_{\mathbf{k}}E_{\mathbf{k-q}} - \epsilon_{\mathbf{k}}\epsilon_{\mathbf{k-q}} - \Delta^2}{E_{\mathbf{k}}^2 - E_{\mathbf{k-q}}^2} \qquad (25)$$

In the limit of $\mathbf{q} \to \mathbf{0}$ the last sum vanishes. The first sum is the contribution due to the quasi-particle excitations and vanishes also at zero temperature, because $E_{\mathbf{k}} > 0$

($\epsilon_F = 0$). Per has calculated the temperature dependence of this term by solving the BCS-energy gap equation. The term does not depend much on the presence of a magnetic field but starts to increase exponential above $0.2\,T_c$. It becomes equal to $\chi_{\text{el}}(\mathbf{0})$ at T_c and is about half this size at $0.7\,T_c$. The temperature dependence is parameterized by the expression ($t = T/T_c$):

$$\chi_{\text{el}}^s(t,\mathbf{0}) = \chi_{\text{el}}(\mathbf{0})\, e^{-6.23403 + 11.4561\,t - 5.28023\,t^2} \qquad (26)$$

At large values of q the superconducting energy gap may be neglected in Eq. (25) and in this case the expression is the same as in the normal case. This modification of the electronic susceptibility and its importance for the RKKY interaction was discussed first by Anderson and Suhl [9] and they estimated that the susceptibility, in the zero temperature limit, develops a maximum at

$$q_d = \left(3\pi k_F^2 \xi^{-1}\right)^{\frac{1}{3}} \qquad (27)$$

Using $k_F \approx 0.2\text{–}0.4\,a^*$ and $\xi = 71$ Å this expression indicates $q_d = 0.14\text{–}0.23\,a^*$. I do not think that this estimate is relevant, as it concerns properties nearly out on the scale of k_F, where large deviations from the behavior of the simple model are expected. A numerical calculation shows that the behavior, in a large regime when $q \ll k_F$, is quite well described by:

$$\chi_{\text{el}}^s(q) = \chi_{\text{el}}(0)\frac{0.99\,q}{q + 1.5\,q_0} \quad ; \quad q_0 = \frac{\pi\Delta}{\hbar v_F} \approx \frac{1}{\xi} \qquad (28)$$

This expression is independent of k_F (as long as $q \ll k_F$). It is not valid at sufficiently small q, where $\chi_{\text{el}}^s(q)$ depends quadratic on q. Fig. 4 shows the numerical result in comparison with the approximate one given by Eq. (28). Band-structure calculations indicate an average Fermi velocity of the order of $2.3 \cdot 10^7$ cm/s $\Rightarrow \xi \approx \hbar v_F / \pi \Delta = 280$ Å or $q_0 \approx 0.002\,a^*$, whereas a direct use of $\xi = 71$ Å gives $q_0 \approx 0.008\,a^*$.
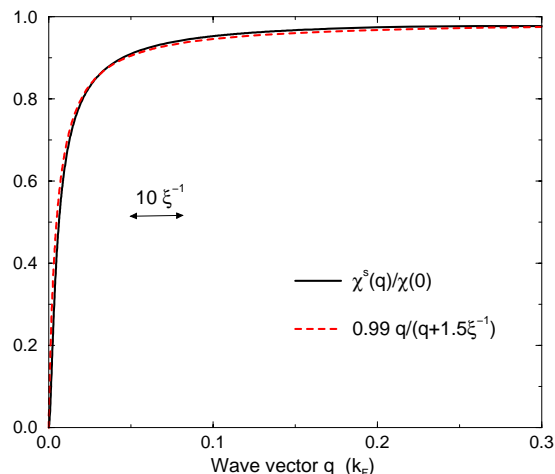
Fig. 4. $\chi_{\text{el}}^s(q)$ has been calculated by linearizing the energies near the Fermi surface: $\epsilon_{\mathbf{k}} = \hbar v_F (k - k_F)$. The density of states is constant and $\Delta = 0.001 \cdot \hbar v_F k_F$. In the regime shown the susceptibility in the normal phase is very close to be a constant. q and ξ^{-1} are in units of k_F, and $\xi^{-1} = 0.001\pi$.

Close to zero wave vector the RKKY-interaction in the normal phase of the Tm system (for $\mathbf{q}$ perpendicular to the c-axis) may be written as $\mathcal{J}(\mathbf{0})[1 - A\,q^2]$. The constant A may be expected to be of the order $5\,(a^*)^{-2}$ (1 would mean at shallow maximum, whereas 5–10 would compare with the order of magnitude of this term in the rare-earth metals, however, the dipole coupling reduces the number in the present system by 4.5, see the caption to Fig. 2; the model has $A = -2.8$). The replacement of $\chi_{\text{el}}(\mathbf{q})$ with $\chi_{\text{el}}^s(\mathbf{q})$ in Eq. (23) only leads to significant changes at $q < 10 \cdot \xi^{-1}$ implying that only the long-wavelength part of the intra-band, $\boldsymbol{\tau} = \mathbf{0}$, term is altered. The analysis of the experiments shows that $\mathcal{J}_s(\mathbf{0})$ in the superconducting phase is close to zero. This result implies that, in this system, $\chi_{\text{el}}(\mathbf{0})$ is the dominating contribution to the RKKY-interaction at zero wave vector, $\mathcal{J}(\mathbf{0}) \approx |j(\mathbf{0})|^2 \chi_{\text{el}}(\mathbf{0})$, occurring because the second, constant, term in Eq. (23) accidentally cancels the inter-band, $\boldsymbol{\tau} \neq \mathbf{0}$, contributions to the first summation term. The $\mathbf{q}$-dependence of $\mathcal{J}(\mathbf{0})[1 - A\,q^2]$, i.e the A term is determined exclusively by the first term in (23). Here the inter-band contributions are expected to be, at least, as important as the $\boldsymbol{\tau} = \mathbf{0}$ term, which is determined by the long-wavelength behavior of the electronic susceptibility. – In the free electron model $\chi_{\text{el}}(q) \simeq \chi_{\text{el}}(0)(1 - q^2/12k_F^2)$ corresponding to a contribution to A of 1 $(a^*)^{-2}$ times $\chi_{\text{el}}(0)/\mathcal{J}(0)$, if k_F is as small as $0.3\,a^*$.– The important point here is that although A may be different in the normal and in the superconducting phase, it is likely that A is still of the order of 5 $(a^*)^{-2}$ also in the superconducting phase. Assuming that the RKKY-interaction in the superconducting phase is $\mathcal{J}(\mathbf{0})[\chi_{\text{el}}^s(q)/\chi_{\text{el}}(0) - A\,q^2]$, then the maximum in this RKKY-function occurs at

$$q_d \simeq \left(\tfrac{4}{3}\,\xi\,A\right)^{-\frac{1}{3}} \qquad (29)$$

(assuming $\xi^{-1} \ll a^*$). Using $A = 5\,(a^*)^{-2}$ and the experimental value of ξ, this expression predicts $q_d = 0.11\,a^*$. The dependence of the actual values of A (or ξ) is slow, if $A\,(a^*)^2$ is changed from 1 to 10 then q_d/a^* is changed from 0.18 to 0.084. This estimate of the ordering wave vector in the superconducting phase can of course only be considered as a rough "order-of-magnitude" estimate. However, the result of the numerical calculation is rather general, as it only depends on the properties of the electrons close to the Fermi surface. In the general case v_F should be replaced by an averaged value, which may correspond to the replacement of the calculated ξ with the experimental one. I think that the estimate may be trusted to such a degree that we may conclude that, **if** the RKKY-coupling in the normal phase of Tm-borocarbide has a (local) maximum at zero wave vector, then the Anderson-Suhl mechanism would shift the maximum out to a value of q which is of the same order of magnitude as observed experimentally. It is possible that it is a "crypto-ferromagnetic" system. On the other hand, the estimate does not exclude the possibility that the maximum in $\mathcal{J}(\mathbf{q})$ at $\mathbf{q} = \mathbf{Q_F}$ is an intrinsic property, also

present in the normal phase. It is rather easy to construct an acceptable model with the maximum at the right position, as shown by the 10-layered model I use in the calculations. The possibility that $TmNi_2B_2C$ may be a crypto-ferromagnetic system has also been discussed by Kulić et al. [10].

The RKKY-interaction is affected by the superconducting energy gap at the Fermi surface. Due to the RKKY exchange the properties of the Fermi surface is also affected by a magnetic ordering, and any change of the Fermi surface may change the superconducting state, as discussed for instance by Amici et al. [11] and in more detail by Nass et al. [12]. A sinusoidally magnetic ordering gives rise to a new periodicity of the system, and the RKKY interaction between the spins of the $4f$ electrons and the conduction electrons leads to energy gaps at the wave vectors $(\boldsymbol{\tau} \pm n \mathbf{Q})/2$, where $\boldsymbol{\tau}$ is a reciprocal lattice vector and $\mathbf{Q}$ is the magnetic ordering vector. The leading order term corresponds to $n = 1$, but the squaring up of the magnetic ordering introduces other odd integer values of n, and the higher-order coupling processes introduce both even and odd values of n. The effects of these so-called superzone boundaries, on the resistivity of the rare-earth metals, were discussed in detail by Elliott and Wedgwood [13], see also the recent discussion by Ellerby et al. [14].

If an energy gap cuts through the Fermi surface the lifting of the degeneracy implies that the states near the gap do not contribute to the creation of Cooper pairs corresponding to a reduction of the "effective density of states" at the Fermi surface appearing in the equation determining the superconducting energy gap. – In a more general formulation (band-model) an energy gap at the Fermi surface is created at a point on the surface, whenever its position differs by the wave vectors $n\mathbf{Q}$ from another point on the surface.– The reduction of the effective density of states is proportional to the size of the energy gap, which by itself is proportional to the amplitude of the magnetic modulation, J_Q [13,12]. The superconducting transition temperature or the energy gap depends exponentially on the (effective) density of states at the Fermi surface:

$$\Delta(0) = 2\omega_D \, \exp\left[-\frac{1}{\mathcal{N}(0)g}\right] \quad (30)$$

and so do the condensation energy $F_s(0) = \frac{1}{2}\mathcal{N}(0)\Delta^2(0)$ and B_{c2}. The precise variation of the effect is not so important in the model calculations presented below. It is the maximum reduction of B_{c2} which is the important quantity. In the calculations I have assumed that the effective density of states in the gap-equation is described by

$$\bar{\mathcal{N}}(J_Q, 0) = \mathcal{N}(0)(1 - \delta) \quad ; \quad \delta = d_A J_Q(A) \quad (31)$$

$J_Q(A)$ is the value of the first harmonic of the Fourier transform of $\langle J_z \rangle$, when $\mathbf{Q} = \mathbf{Q}_A$. The effect seems only to be important in the Q_A-modulated phase, probably because the superzone gaps created by this ordering destroy important nesting features at the Fermi surface, whereas the energy gaps produced by the Q_F-ordering are much more harmless to the effective density of states. The scaling of the density of states introduced by Eq. (31) then implies:

$$\frac{T_c}{T_c^0} = \frac{B_{c2}}{B_{c2}^0} = \exp\left[\frac{\delta}{1-\delta}\ln\left(\frac{\Delta(0)}{\omega_D}\right)\right] \simeq \exp\left[-\frac{2\delta}{1-\delta}\right] \quad (32)$$

(using ω_D of the order of 13 meV, the right value is not important). The final value of the fitting parameter is

$$d_A = 0.053 \quad (33)$$

$J_Q(A)$ is of the order of 4 in the low temperature limit, which implies a relative reduction of the effective density of states by 20% ($\delta = 0.2$) and of B_{c2} by 40%. The magnitude of the energy gaps created by the RKKY coupling is very uncertain. The free electron model suggests that the energy gaps may be of the order of 20 meV when the magnetic moments are saturated (ferromagnetic), $[= 2J\{\mathcal{J}(0)/2\mathcal{N}(0)\}^{1/2}]$, i.e. of the order of 10 times the superconducting energy gap.

IV. THE PHASE DIAGRAM OF $TmNi_2B_2C$

The different magnetic phases to be considered are the paramagnetic (P) and the two ordered phases at $\mathbf{Q} = \mathbf{Q}_F$ or $\mathbf{Q}_A$, the F or A phase, respectively. The three magnetic phases may occur while the electronic system is either in the normal (N) or in the superconducting state (S). Hence, we need to consider 6 different phases of which only one (NF) does not seem to appear. The phase diagram is constructed using a number of parameters, which are

- Magnetic coupling parameters: The 5 crystal-field parameters in Table I. The demagnetization factor $D^{zz} = 0.76$. The three exchange parameters, $\mathcal{J}(0) \simeq \mathcal{J}(\mathbf{Q}_F) = 8.6 \ \mu eV$ and $\mathcal{J}(\mathbf{Q}_A) = 15.0 \ \mu eV$.

- Superconductor parameters: $T_c = 11.5$ K (the use of this value instead of 11 K should not be taken too literally). $B_{c2}(0) = 65$ kG, where the two parameters determine $B_{c2}(T)$ as given by Eq. (14). The condensation-energy parameter $1.16(2\kappa_F^2 - 1) = 90$ or $\kappa_F = 6.27$.

- The parameters describing the effects of the interactions between the magnetic and superconducting electrons: The two-ion coupling parameter in the superconducting state,

$$\mathcal{J}_s(\mathbf{0}) = \mathcal{J}(\mathbf{0})\Big(1 - \alpha\big[1 - \chi_{el}^s(t,0)/\chi_{el}(0)\big]\Big) \quad (34)$$

The susceptibility ratio is given by Eq. (26) and in the final fit $\alpha = 1$. The RKKY energy-gap parameter $d_A = 0.053$ determining the reduction of the effective density of states in the SA-phase, $\delta = d_A J_Q(A)$.

Out of these $9 + 3 + 2 = 14$ parameters the construction of the phase diagram has lead to the determination of $3 + 2 + 2 = 7$ parameters.

A. The SP–NP transition

The transition between the normal and the superconducting state, while the magnetic system stays paramagnetic, determines the 2 (3) superconducting parameters, $B_{c2}(0)$ and κ_F (and T_c). The calculation of the position of this transition requires two more of the remaining 5 fitting parameters, namely $\mathcal{J}(\mathbf{0})$ and α, which are both determined from the SF–SP transition, in combination with the assumption of $\mathcal{J}(\mathbf{0}) \simeq \mathcal{J}(\mathbf{Q}_F)$, which may be expected to be true to within $\pm 5\%$. I may add that it is not the two coupling parameters themselves but their difference $\mathcal{J}(\mathbf{0}) - \mathcal{J}_s(\mathbf{0})$, which is the significant parameter in the calculations.
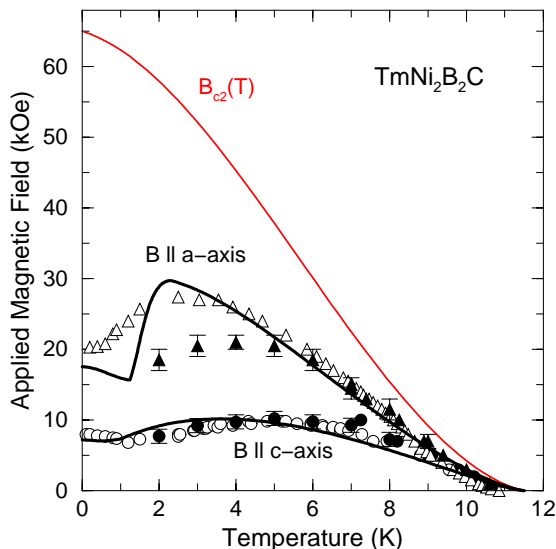
Fig. 5. The transition between the superconducting and the normal phase, when applying a field parallel or perpendicular to the c-axis. The closed symbols show the experimental results of Cho *et al.* [3], and the open ones are the results of Don Naugle and Daya Rathnayaka [15]. The solid lines are the calculated results. The thin (red) line shows $B_{c2}(T)$ used in the fit, as explained in the text.

I have tried to consider the free energy accounts at the SP–NP transition, when the field is applied along the c-axis at 1.6 K (above the SF-phase). Although the temperature is low, the magnetic entropy is still important, but it may be estimated assuming the crystal-field system to be determined alone by the ground-state doublet. The diagonal J_z matrix-elements between the two

state vectors are $+M_z$ and $-M_z$, where $M_z = 3.893$, however, the use of a slightly larger effective value of about 4.1 gives a better estimate of the magnetization (and thus also of the entropy). At 1.6 K the transition occurs at the field $B = 8.557$ kG implying $B_i = 9.981$ kG and with $B_{c2}(T) = 59.92$ kG the free energy of the superconductor is $F_s/N = -44.3$ μeV (per Tm-ion). Just below the transition $\langle J_z \rangle = 2.808$ and just above $\langle J_z \rangle = 3.592$. Hence, there is a jump in the magnetic moment of 0.9 μ_B at the transition, which is **not** observed in the experiments of Cho *et al.* [3]. The Zeeman and dipolar energies are rather large: $-g\mu_B B\langle J_z \rangle + 2\pi DM^2/N = -119.5$ μeV below the transition and above -137.6 μeV (using $D = 0.76$). Finally, the exchange energy is zero below the transition $[\mathcal{J}_s(\mathbf{0}) = 0]$ whereas in the normal phase $-\frac{1}{2}\mathcal{J}(\mathbf{0})\langle J_z \rangle^2 = -55.1$ μeV. In the simplified model the internal energy of the crystal-field Hamiltonian is zero, but the entropy is changed. The value $\langle J_z \rangle = 2.808 = 4.1(n_0 - n_1)$, in the superconducting phase corresponds to the population factors $n_0 = 0.842$ and $n_1 = 1 - n_0 = 0.158$. These numbers agree quite well with that derived from $H^{\mathrm{eff}} = 4.05$ kOe, which gives rise to a splitting of the doublet by 0.225 meV. The entropy contribution to the free energy is $-ST = k_B T(n_0 \ln n_0 + n_1 \ln n_1) = -60.2$ μeV. In the normal phase the corresponding numbers are $n_0 = 0.937$, $n_1 = 0.063$, $H^{\mathrm{eff}} = 7.33$ kOe (and thus an energy splitting of the doublet by about 0.41 meV) implying $-ST = -33.0$ μeV. The different contributions to the energy differences between the superconducting and the normal phase are then (in units of μeV): Condensation: -44.3; Exchange: 55.1; Zeeman and dipolar: 18.1; Entropy: -27.2 (-28.9), which numbers add up to zero (if using the right value in the bracket for the entropy term). At this temperature, the gain in Zeeman and dipolar energy is roughly out-balanced by the free-energy change due to the reduction of the entropy. Hence the loss of the superconducting condensation energy by about 44.3 μeV is compensated for by the gain in exchange energy due to the jump in $\mathcal{J}(\mathbf{0})$ by 8.6 μeV.

Figure 5 shows the final fit to the experiments of Cho *et al.*. The experimental results of Don Naugle and Daya Rathnayaka are added after the fit was made! (The value of the demagnetization factor influences the results, and it is therefore important that Don Naugle and Daya Rathnayaka give us a rough estimate of the demagnetization factor of the sample they have used). The calculation, in the case where the field is perpendicular to the c axis, is made with the field along the a-axis, [100], however, the anisotropy is insignificant below 20 kOe and the maximum at 2.4 K in the [110] case is only about 2 kOe higher than in the [100] case. In the calculations the anisotropy in the position of the transition is due exclusively to the anisotropy of the magnetic system. The magnetic moment induced by the field is much smaller in the a-axis than in the c-axis case, thus the superconducting condensation energy has to be reduced more before it may be compensated by the gain in exchange energy.

– At 2.4 K the critical field is 29.61 kG and the two values of $\langle J_x \rangle$ is 1.4653 and 1.5801 corresponding to a jump in the magnetic moment of 0.13 μ_B. The condensation energy is determined by $B_i = 32.34$ kG and $B_{c2} = 55.79$ kG, or $F_s/N = -9.8$ μeV, and the exchange energy in the normal phase has nearly the same value $-\frac{1}{2}\mathcal{J}(\mathbf{0})\langle J_x \rangle^2 = -10.7$ μeV.– Considering that the fit is determined (effectively) by only two parameters, $B_{c2}(0)$ and κ_F, leading to a reasonable result for both ones, the final result is convincing. The mechanism for the transition must be the right one. The problem left is that the transitions are predicted to be strongly first-order ones with jumps in the values of the magnetic moments (rather small in the a-axis case, but certainly observable in the c-axis case). The experiments of Cho et $al.$ [3] indicate that the transitions are continuous with a jump in the derivative of the magnetization.
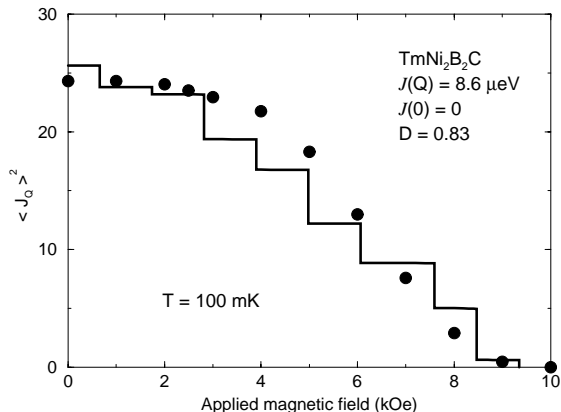
Fig. 6. The experimental points are the total magnetic scattering intensities observed by Morten (adding the intensities of the different scattering peaks). The experimental intensity scale has been adjusted so to fit the calculated results shown by the solid line. The theoretical results are derived using a 20 layered structure instead of the 10 layered one, in order to get a more smooth result.

B. The SF–NP and SA–SP transitions

The study by Morten et $al.$ of the SF-phase, when applying a field along the c-axis, has been used for determining two parameters: $\mathcal{J}(\mathbf{Q}_F) = 8.6$ μeV is simply determined by the transition temperature $T_N = 1.52$ K at zero field. The other parameter is the amount by which the superconducting electrons suppresses $\mathcal{J}(\mathbf{0})$. The small value of Q_F implies that in a normal metal $\mathcal{J}(\mathbf{0})$ may only be up to 5% smaller than $\mathcal{J}(\mathbf{Q}_F)$, and in this case the c-axis modulated F-phase would change into the paramagnetic (ferromagnetic) phase at a critical field of the order of 0.3 kOe. However, in the low temperature limit the SF-phase is observed to exist up to a field of the order of 10 kOe, which is only possible if $\mathcal{J}(\mathbf{0})$ is strongly reduced by the superconducting electrons. The magnetic intensity measurements at 100 mK, Fig. 53 in

Morten's thesis, have been used for deriving that $\alpha \simeq 1$ or $\mathcal{J}(\mathbf{0}) = 0$ in the superconducting phase. The fit of the intensities is shown in Fig. 6. Notice that the reduction of the oscillating moment goes stepwise, by the flipping of one moment in the period per step. This means that the SF-SP transition at a certain temperature, very quickly below T_N, becomes a first-order one. At T_N, or when the field is applied perpendicular to the c axis, the transition is of second order.
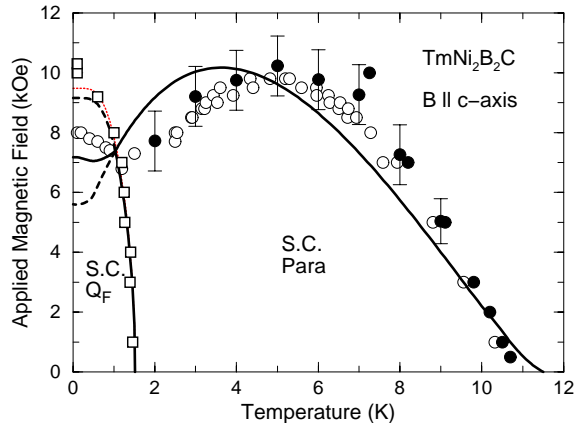
Fig. 7. The phase diagram of the superconducting and magnetic phases in TmNi$_2$B$_2$C in the presence of an applied field in the c-direction. The open and closed circles show the experimental results from, respectively, Ref. [15] and [3]. The squares show the experimental results of Morten. The solid lines are the calculated phase lines and the dashed ones are extrapolations of the phase lines. The thin (red) dashed line is the result obtained using $D = 0.85$ rather than 0.76.

When making the calculations shown in Fig. 6, I have assumed that the system stays in the superconducting phase (the reduction factor α is assumed constant). The F-phase should not be stable outside the superconducting state (at fields larger than 0.3 kOe). On the other hand the superconducting state may take advantage of the energy gain due to the presence of the F-phase in comparison with the SP-phase. This implies, as shown in Fig. 7, that the SF–NP phase line in the c-axis case is pushed towards higher field values in comparison with the SP–NP line (the dashed line). However, this advantage becomes smaller the smaller the oscillating moment is, and the transition should be a first-order one, where the magnetic intensity suddenly jumps to zero. This does not agree with Morten's measurements, as he has seen a tail of the intensities continuing into the normal phase, assuming that the measurements in Ref. [15] are correct in showing that the normal phase appears above 7–8 kOe. My only explanation is that a non-uniform distribution of the demagnetization field may create small volumes in the sample where the effective D is nearly 1, in which volumes the SF-phase may stay stable up to higher values of the applied field. The calculated SF–SP phase line in the superconducting phase agrees well with the mea-

surements of Morten, which adds to the credibility of the value of α derived in Fig. 6.

The phase diagram in the a-axis case is shown in Fig. 8. This phase diagram would have been qualitatively similar to the one shown in Fig. 7, if not for the appearance of the phase with the magnetic ordering wave-vector $\mathbf{Q}_A$. One difference is that the field perpendicular to the c-axis has a very weak effect on the c-axis modulated structure, and the F-phase would be stable up to very high fields (of the order of 30–40 kOe) in a normal magnetic system. The calculated SF–SP phase-line is therefore nearly vertical in Fig. 8.

The last two phases to be considered are the SA and NA phases. The stability of these two phases is established in terms of the two remaining fitting parameters $\mathcal{J}(\mathbf{Q}_A)$, determining the Néel temperature of this phase in the normal state, and d_A, determining how much this ordering disturbs the superconducting phase. The value of $\mathcal{J}(\mathbf{Q}_A) = 15$ μeV corresponds to a Néel temperature of 2.67 K, as indicated by the dashed line in Fig. 8, and in the zero-temperature limit the NA-phase should be stable up to a field of 45 kOe. In order to determine the fit, I started out by assuming the Q_A-phase to be unstable in the superconducting case. Then $\mathcal{J}(\mathbf{Q}_A)$ was adjusted so that the NA-phase would appear at about 12–13 kOe at zero temperature. The position of this transition is very sensitive to any change of $\mathcal{J}(\mathbf{Q}_A)$, implying that this parameter can not possibly be much larger as that would drive the transition down to zero field, and the NA and possibly also the SA phase would appear in, and modify appreciably, the c-axis phase diagram. The final value of this parameter implies that the normal A-phase is just at the threshold of being stable at the SF–NP phase-line in the c-axis diagram. It is still an open question, whether this phase is present in the c-axis case, possibly in a small pocket around the SF–NP phase-line, and this question has to be settle by an experimental investigation. The next step in the fitting procedure was to reduce d_A to a value where the A-phase started to be stable also in the superconducting state. A fine tuning of d_A to the value of 0.053 led to the calculated a-axis phase diagram in Fig. 8.

The a-axis phase diagram has been investigated by neutron diffraction experiments up to a maximum field of 18 kOe. In the low temperature limit scattering intensities due to the Q_F-ordering were observed up to a field of about 14 kOe. The Q_A-ordering is observed to appear above about 9 kOe and to exist still at the maximum field of 18 kOe. In Fig. 8 the dark-gray (magenta) area indicates the occurrence of the A-phase, and the gray (cyan) area is the one where the two magnetic phases are observed to coexist. The light-gray (yellow) area indicates the one in which weak scattering intensities due to the Q_A ordering are still observable. The latter results are obtained whilst heating the sample at a constant field. The squares denote the temperatures at which the Q_A-scattering intensities are half the zero-temperature values, at a constant field, corresponding to

the points where the intensities are rapidly declining with increasing temperature. These points are lying close to the first-order phase-lines bounding the areas in which the Q_A phase is calculated to exist.
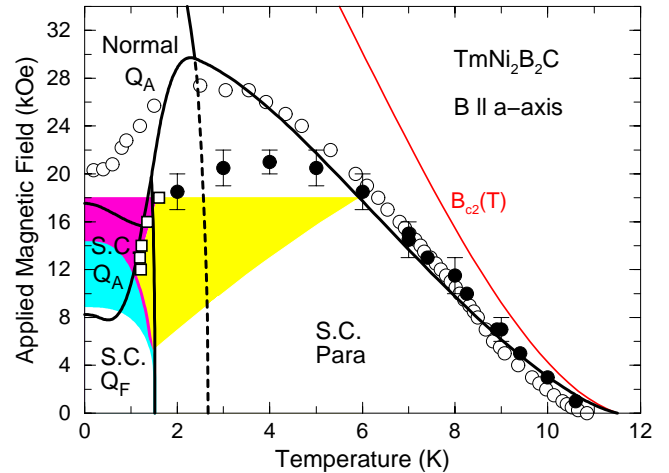
Fig. 8. The phase diagram of the superconducting and magnetic phases in TmNi$_2$B$_2$C, when the field is applied perpendicular to the c-direction. The open and closed circles show the experimental results from, respectively, Ref. [15] and [3]. The squares and the hatched areas indicate the experimental results of Katrine, as explained in the text. The solid lines are the calculated phase lines and the dashed one is the extrapolation of the NA-NP phase line.

Hysteresis effects are expected at the different first-order transitions, but the light-gray area in Fig. 8 extends far beyond that, which may possibly be explained by usual hysteresis effects. In the a-axis configuration the demagnetization field is small and a possible inhomogeneous distribution of this field is unimportant. The variations in the magnetic field may help to smear out the transitions but this effect is weak, as indicated by Fig. 3, probably less than 0.5 kOe. The remaining possibility is the effects due to a spatial variation of the superconducting order-parameter. Within the core radius ξ of the flux lines the electrons are normal, and in these volumes the Q_A ordering may survive in the paramagnetic phase, as considered by Per. This effect may possibly explain a part of the observed light-gray area, but it is still difficult to understand how a substantial part of the light-gray area in Fig. 8 may cover temperatures at which the Q_A ordering is unstable also in the normal phase (this stability line is indicated by the dashed line in the figure). The presence of normal electrons in the cores of the flux-lines may also be the reason why the magnetic moments are observed to change continuously at the SP – NP phase lines. In the c-axis case where this jump is calculated to be quite large, the non-uniformity of the demagnetization field may be just as important.

[1] J. W. Lynn, S. Skanthakumar, Q. Huang, S. K. Sinha, Z. Hossain, L. C. Gupta, R. Nagarajan and C. Godart, Phys. Rev. B **55**, 6584 (1997).

[2] U. Gasser, P. Allenspach, F. Fauth, W. Henggeler, J. Mesot, A. Furrer, S. Rosenkranz, P. Vorderwisch and M. Buchgeister, Z. Phys. B **101**, 345 (1996).

[3] B. K. Cho, M. Xu, P. C. Canfield, L. L. Miller and D. C. Johnston, Phys. Rev. B **52**, 3676 (1995).

[4] G. J. Bowden and R. G. Clark, J. Phys. C **14**, L827 (1981).

[5] S. V. Shulga, S.-L. Drechsler, G. Fuchs and K.-H. Müller, Phys. Rev. Lett. **80**, 1730 (1998).

[6] K. D. D. Rathnayaka, A. K. Bhatnagar, A. Parasiris and D. G. Naugle, Phys. Rev. B **55**, 8506 (1997).

[7] M. Crisan, *Theory of superconductivity*, (World Scientific, Singapore, 1989), Eqs. (7.26) and (7.60).

[8] J. Jensen and A. R. Mackintosh, *Rare Earth Magnetism: Structures and Excitations* (Clarendon Press, Oxford, 1991).

[9] P. W. Anderson and H. Suhl, Phys. Rev. **116**, 898 (1959).

[10] M. L. Kulić, A. I. Buzdin and L. N. Bulaevskii, Phys. Lett. A **235**, 285 (1997).

[11] A. Amici, P. Thalmeier and P. Fulde, cond-mat/9811226 (1998).

[12] M. J. Nass, K. Levin and G. S. Grest, Phys. Rev. Lett. **46**, 614 (1981).

[13] R. J. Elliott and F. A. Wedgwood, Proc. Phys. Soc. **81**, 846 (1963).

[14] M. Ellerby, K. A. McEwen and J. Jensen, Phys. Rev. B **57**, 8416 (1998).

[15] D. G. Naugle, K. D. D. Rathnayaka, K. Clark and P. C. Canfield (to be published and private communication).